

Study to Achieve Stable VNA Measurements Using 500-750 GHz Quasi-Optical Setup

Downloaded from: https://research.chalmers.se, 2026-11-27 10:30 UTC

Citation for the original published paper (version of record):

Hellmich, D., Dileep Jatkar, K., Rodilla, H. (2026). Study to Achieve Stable VNA Measurements Using 500-750 GHz Quasi-Optical Setup. 56th European Microwave Conference, EuMC 2026. http://dx.doi.org/10.23919/EuMC69230.2026.11748148

N.B. When citing this work, cite the original published paper.

research.chalmers.se offers the possibility of retrieving research publications produced at Chalmers University of Technology. It covers all kind of research output: articles, dissertations, conference papers, reports etc. since 2004. research.chalmers.se is administrated and maintained by Chalmers Library

(article starts on next page)

Study to Achieve Stable VNA Measurements Using 500-750 GHz Quasi-Optical Setup

Daniel Georg Hellmich[1], Kasturie Dileep Jatkar, Helena Rodilla
Terahertz and Millimetre Wave Laboratory, Chalmers University of Technology, Gothenburg, Sweden
[1]hellmich@chalmers.se

***Abstract* — A quasi-optical S-parameter measurement system in the 500–750 GHz (WM-380) frequency range for high-loss samples was characterized for its dynamic range and stability using Allan deviation. The system provides a dynamic range of more than 114 dB in the 630–690 GHz frequency range. Allan deviation was used to find the highest stability and sensitivity, as a trade-off between mitigating noise and drift, by finding the right combinations of intermediate frequency (IF) bandwidth of the vector network analyzer and number of averaged measurements. We observe that a 600-µm-thick water sample, measured with an IF bandwidth of 100 Hz with 16 averages yields a stability better than 0.01 dB.**

***Keywords* — Allan deviation, high-loss samples, THz, Quasi-optics, VNA, Water.**

I. Introduction

The high absorption of terahertz (THz) waves by liquid water, with an absorption coefficient of 240 cm^{-1} at 1 THz [1], [2], makes spectroscopy measurements of aqueous solutions extremely challenging. Reliable measurements of the dielectric properties of highly absorbing materials require methods that provide good stability, sensitivity, and high signal-to-noise ratio (SNR). The most common methods to address this challenge are based on time-domain spectroscopy (TDS) [3], [4]. Commercial THz-TDS systems emit broadband THz pulses pumped with a femtosecond laser. A Fourier transformation converts the time-domain measurement to frequency-domain, providing the sample's absorption spectrum. Due to low optical-to-THz conversion efficiency, this technique typically has a power level in the order of hundreds of µW distributed over the wide THz spectrum, which complicates spectroscopy of lossy samples like aqueous solutions. In particular, the thickness of the sample is a limitation in these measurements, where it is typically restricted to a maximum of around 200 µm since the quality of the transmitted signal is limited by the dynamic range of the system. On the one hand, thin samples provide higher transmitted signals but are strongly affected by Fabry-Perot reflections and irregularities in the sample geometry [5]. On the other hand, thick samples lead to longer interaction time and higher phase accumulation, which makes them beneficial for determining the real part of the permittivity, although the signal decreases for high-loss materials. Despite their advantages in the determining the complex dielectric properties, limited work has been done on thick samples [6].

To address these challenges, we propose to take advantage of the high dynamic range of vector network analyzer (VNA) based S-parameter measurements for the THz characterization of aqueous solutions. Advances in electronics now enable S-parameter measurements as high as 1.5 THz [7] by combining a VNA with frequency extenders. This system, combined with a quasi-optical setup, allows for a low-loss, non-destructive material characterization system through S-parameter measurements. Moreover, the use of ultra-gaussian corrugated horn antennas provides a defined gaussian beam, allowing for accurate extraction of the sample's permittivity [8].

For aqueous solutions, the detection of a mere 0.05% change in the refractive index requires the ability to distinguish at least 0.024 dB in the amplitude of S-parameters, entailing high measurement stability. In this paper, we systematically investigate the dynamic range, and the impact of random noise and drift on the stability of the system to evaluate its capabilities for THz characterization of aqueous solutions and other high-loss samples.

II. Measurement Setup

The measurement setup consists of a VNA (Keysight PNA-X N5242B), WM-380 frequency extenders from Virginia Diodes (500–750 GHz), ultra-gaussian corrugated horn antennas with 99.88% gaussicity from Thomas Keating, and a quasi-optical setup comprising four off-axis parabolic mirrors and a sample cell (Fig. 1).

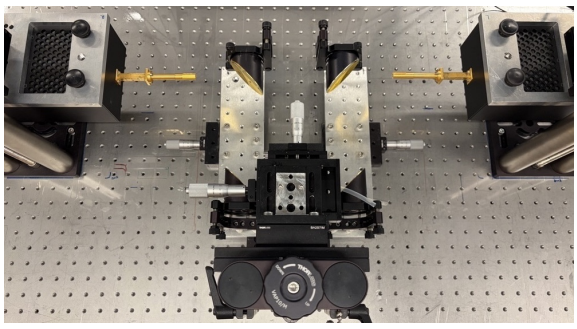

Fig. 1. Photograph of the quasi-optical measurement system.

The free-space THz beam leaves the VNA extender working as an emitter through the antenna in the form of a diverging gaussian beam (Fig. 2). The beam is then collected and reflected by a gold-coated off-axis parabolic mirror with a focal length of 76.2 mm producing a collimated beam. This beam travels a distance of 150 mm after which it is focused

onto the sample cell by a second mirror identical to the previous one. After interacting with the sample, a symmetric quasi-optical system is used to collect the beam back to the extender working as the receiver. The beam diameter at the focus is roughly 2.8 mm. The two mirrors at each side of the sample cell are physically grouped into two sets and mounted on a breadboard equipped with micro-manipulators to allow precise manipulation during the alignment.

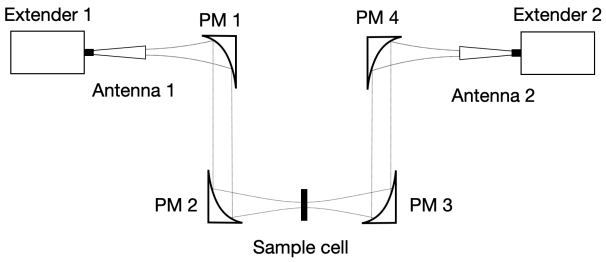

Fig. 2. Schematic of the quasi-optical measurement system.

The VNA with frequency extenders was calibrated at the waveguide flanges (before the antenna) using Short-Open-Load-Through calibration with 801 frequency points and an intermediate frequency (IF) bandwidth of 300 Hz prior to the system alignment. The extender 2 was fixed in its final position, while the extender 1 was moved during calibration and the alignment procedure. The setup was aligned by placing a visible laser to replicate the path of the THz beam. A demountable liquid cell from Specac Ltd was mounted on a 3-axis translation stage and placed at the beam focus (Fig. 2). The liquid cell consists of two metallic plates pressed against a cell nest with a neoprene gasket, custom-made TOPAS windows, and a polylactic acid spacer. A syringe, connected to the filling ports of the cell through tubing, was used to fill the liquid cell during the experiments. The sample cell was centered with the help of the laser beam and by real-time time-domain information of all S-parameters.

III. Measurements

A. System characterization

The S-parameters of the aligned quasi-optical system before introducing the liquid cell are shown in Fig. 3. A transmission of around -4 dB was obtained in the upper half of the frequency band before decreasing above 740 GHz due to limited output power of the frequency extenders in this region. The lesser transmission of about -10 dB in the lower half of the frequency band is due to the frequency-dependent behavior of the corrugated horn antennas. The sharp dip in the transmission at 557 GHz corresponds to a strong absorption line from water vapor present in the atmosphere [2]. Since the frequency extender used at port 2 provides a higher output power, only S_{12} will be considered in the following.

The noise floor of the system was determined by measuring the transmission with a strong absorber placed at the position of the sample cell in the optical path. The measurement was

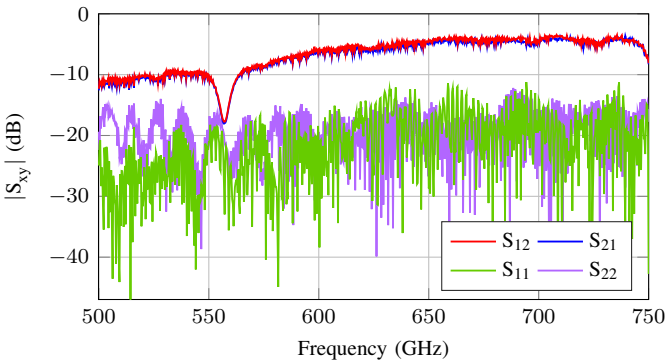

Fig. 3. Measured S-parameters of the waveguide-flange calibrated quasi-optical system after alignment.

conducted with an IF bandwidth of 1 Hz to achieve highest sensitivity of the system without averaging. The dynamic range of the system, defined as the difference between the maximum transmission and the sensitivity limit, is shown in Fig. 4. As

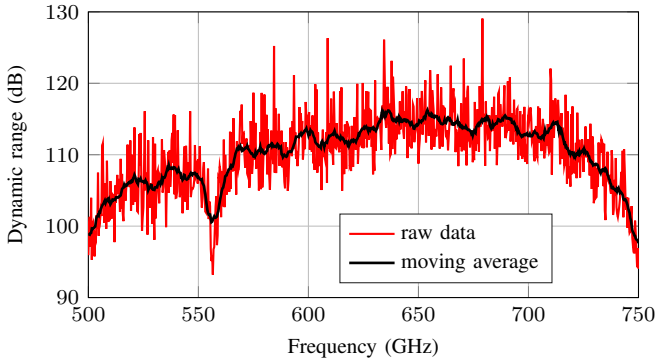

Fig. 4. Dynamic range determined as difference of maximum transmission and maximum sensitivity of the system. Raw data is shown together with a moving average over 20 frequency points.

expected, the sensitivity and thus the dynamic range decreases at the edges of the frequency range since the output power of the frequency extenders is lower at the edges of their operating frequency band. The maximum dynamic range of >114 dB is achieved for the frequency range 630–690 GHz. Within this frequency range, our system including the frequency extenders, antennas, and the quasi-optical path exhibits a larger dynamic range than the typical dynamic range specified for the frequency extenders alone measured at an IF bandwidth of 10 Hz with 10 averages. This measurement condition is equivalent to the measurement settings of our system for maximum sensitivity [9].

B. System Drift

The drift of the system, including thermal drift of the electronics of the VNA and frequency extenders, as well as the effect of changes in atmospheric conditions, was examined for three hours with a 600-µm-thick layer of deionized water in the sample cell. In Fig. 5 the normalized amplitude of each S_{12} measurement over three hours is shown. The plots show the

drift of the system for three arbitrarily chosen frequency points. The magnitude of S_{12} exhibits changes of up to 0.1 dB over 1 hour at a fixed frequency point. The surrounding temperature was ∼23 °C and the relative humidity decreased from 27% to 23% during the time period of 3 hours.

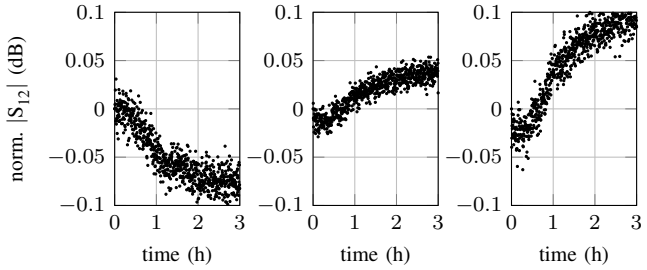

Fig. 5. Measured magnitude of S_{12} normalized to the first measured value over 3 hours with 100 Hz IF bandwidth at three arbitrary frequency points.

C. System Stability

The system was evaluated for its suitability in accurate characterization of high-loss samples, where maximum sensitivity and dynamic range are required. The sensitivity of the measurement system is impacted by the choice of the IF bandwidth of the VNA as well as the number of averages per measurement. On the one hand, lower IF bandwidths decrease the broadband noise in the receiver which can not only increase the dynamic range but also the SNR, which prevents the loss of information of the signal due to noise [9]. Decreasing the IF bandwidth by a factor of 2 increases the SNR by 3 dB, but the sweep time also increases. This increase in sweep time is proportional to the change in IF bandwidth for values below 300 Hz, while for larger IF bandwidths the increase in sweep time is lesser. On the other hand, averaging over consecutive sweeps improves the SNR by 3 dB for doubling the number of averages, which doubles the measurement time [10]. As shown in the previous section, the system exhibits measurable drift. Hence, a trade-off between noise mitigation by averaging or decreasing IF bandwidth, and drift as a consequence of the increased measurement time must be found by selecting the right combination of IF bandwidth and number of averages.

To estimate the stability of our system, we use the Allan deviation (AD) defined as

$$\sigma_A(\tau) = \sqrt{\frac{\sum_{i=1}^{N-1}(\bar{T}_{i+1} - \bar{T}_i)^2}{2(N-1)}} \qquad (1)$$

where $\bar{T}$ is the average of consecutive measurements over time intervals τ, and N is the number of such averaged sets. This technique, originally developed to measure the frequency stability of clocks [11], can also be used to determine the stability of the system over time. It allows to distinguish effects from different types of noise and drift. The minimum value for AD denotes the minimal variability between consecutive sets of measurements, thus, providing a good number of averages which reduces the impact of random noise observed for low number of averages, and the impact of drift, often observed for long measurement times due to high number of averages.

To recognize which combinations of IF bandwidth and averages provide the most stable conditions, we performed transmission measurements through our sample cell with 200-µm and 600-µm-thick water layers for different IF bandwidths. The AD, as the arithmetic mean of σ_A over the frequency range 630–690 GHz, region with the highest dynamic range (Fig. 4), is plotted against IF bandwidth and number of averages in the color maps shown in Fig. 6 and Fig. 7. The y-axis of the plots denotes the IF bandwidth. Typically, the measurement time is plotted along the x-axis for AD plots, however, due to varying measurement times for each IF bandwidth, we show the number of averages in logarithmic scale along the x-axis to improve readability. Within each row, the measurement time increases with the number of averages. The dark blue regions denote low AD implying higher stability, while higher AD (yellow) indicates presence of random noise (top-left) or drift (bottom-right) in the measurement.

The AD for the 200-µm-thick water sample is shown in Fig. 6. The areas with the darkest shade of blue in

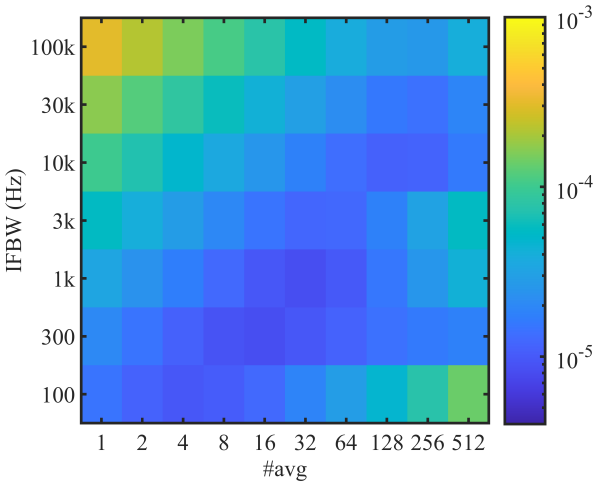

Fig. 6. AD (denoted by logarithmic color bar) vs. IF bandwidth (IFBW) and number of averages for a 200 µm thick water sample.

each row which correspond to the lowest AD represent the optimal number of averages for the respective IF bandwidth. The measurement times for these lowest AD values are approximately the same for different IF bandwidths considering the differences in sweep times and number of averages. This region of optimal conditions yields a stability better than 0.01 dB. With an IF bandwidth of 100 Hz, four averages are required to achieve the lowest AD which corresponds to a measurement time of 58 s. For a higher number of averages the drift of the system deteriorates the averaged transmission measurement. As the IF bandwidth increases, the number of averages required for a small AD increases.

For a 600-µm-thick water sample (Fig. 7), we observe that the lowest AD for an IF bandwidth of 100 Hz is yielded by

averaging 16 transmission measurements, which corresponds to a measurement time of 218 s. Beyond 16 averages for 100 Hz IF bandwidth the AD increases, indicating that the drift of the system outweighs the improvement in signal quality through averaging. The stability of the system for the lowest AD at all considered IF bandwidths was found to be $<$0.03 dB in the range between 630–690 GHz. For IF bandwidths $\leq$10 kHz with their corresponding best number of averages, the stability is better than 0.01 dB.

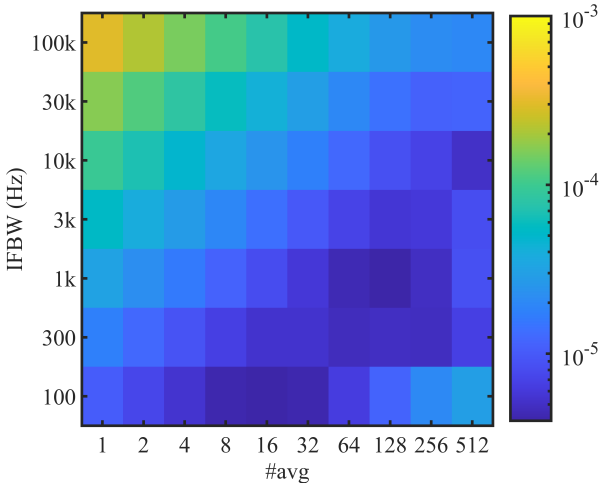

Fig. 7. AD (denoted by logarithmic color bar) vs. IF bandwidth (IFBW) and number of averages for a 600 µm thick water sample.

IV. Conclusion

In this paper, we studied the dynamic range and stability of a quasi-optical THz system to be used for the characterization of high-loss liquid samples between 500 and 750 GHz. The Allan deviation was used to find the combinations of IF bandwidth and number of averaged measurements that provide highest stability. For a water sample of 200 µm thickness, the stability for all presented IF bandwidths with their respective optimal number of averages is found to be better than 0.01 dB. For a 600-µm-thick sample, stability better than 0.01 dB is achieved for IF bandwidths $\leq$10 kHz with the corresponding optimal number of averages. This stability allows to detect changes of 0.05% in the refractive index. In summary, we demonstrate that the VNA-based quasi-optical setup is a promising method for the investigation of aqueous solutions at THz frequencies.

V. Acknowledgment

The authors would like to thank Dr Harrison Lees for support with the real-time time-domain techniques used for the alignment and Jonathan Westin for machining parts for the setup. The measurements were carried out in the Kollberg Laboratory, at the Chalmers University of Technology, Gothenburg, Sweden. This work was supported by the Swedish Research Council (Vetenskapsrådet) under the grant 2024-01981.

References

[1] P. Siegel, "Terahertz Technology in Biology and Medicine," *IEEE Transactions on Microwave Theory and Techniques*, vol. 52, no. 10, pp. 2438–2447, Oct. 2004.

[2] I. Gordon et al., "The HITRAN2020 molecular spectroscopic database," *Journal of Quantitative Spectroscopy and Radiative Transfer*, vol. 277, p. 107 949, Jan. 2022.

[3] J. Kölbel, W. Schirmacher, E. Shalaev, and J. A. Zeitler, "Terahertz dynamics in the glycerol-water system," *Phys. Rev. B*, vol. 107, p. 104 203, 10 Mar. 2023.

[4] E. M. Adams, O. Lampret, B. König, T. Happe, and M. Havenith, "Solvent dynamics play a decisive role in the complex formation of biologically relevant redox proteins," *Phys. Chem. Chem. Phys.*, vol. 22, pp. 7451–7459, 14 2020.

[5] W. Withayachumnankul, B. M. Fischer, and D. Abbott, "Material thickness optimization for transmission-mode terahertz time-domain spectroscopy," *Optics Express*, vol. 16, no. 10, p. 7382, May 2008.

[6] F. Novelli, "Terahertz spectroscopy of thick and diluted water solutions," *Optics Express*, vol. 32, no. 7, p. 11 041, Mar. 2024.

[7] D. Koller, S. Durant, C. Rowland, E. Bryerton, and J. Hesler, "Initial measurements with WM164 (1.1–1.5THz) VNA extenders," in *2016 41st International Conference on Infrared, Millimeter, and Terahertz waves (IRMMW-THz)*, Copenhagen, Denmark: IEEE, Sep. 2016, pp. 1–2.

[8] M. Mrnka, R. Appleby, and E. Saenz, "Accurate S-Parameter Modeling and Material Characterization in Quasi-Optical Systems," *IEEE Transactions on Terahertz Science and Technology*, vol. 12, no. 2, pp. 199–210, Mar. 2022.

[9] M. Hiebel, *Fundamentals of Vector Network Analysis*. Rohde & Schwarz, 2008.

[10] J. A. Jargon, A. A. Koepke, and P. D. Hale, "Investigating the Effects of IF Bandwidth and Averaging on Calibrated Scattering-Parameter Measurements," in *2019 93rd ARFTG Microwave Measurement Conference (ARFTG)*, Boston, MA, USA: IEEE, Jun. 2019, pp. 1–4.

[11] D. Allan, "Statistics of atomic frequency standards," *Proceedings of the IEEE*, vol. 54, no. 2, pp. 221–230, 1966.